Site-Directed Mutagenesis and Spectroscopic Characterization of Human Ferrochelatase: Identification of Residues Coordinating the [2Fe-2S] Cluster†

Brian R. Crouse,‡ Vera M. Sellers,§ Michael G. Finnegan,‡ Harry A. Dailey,§ and Michael K. Johnson*,‡

Department of Microbiology, Department of Chemistry, and Center for Metalloenzyme Studies, University of Georgia, Athens, Georgia 30602

Received August 12, 1996; Revised Manuscript Received October 7, 1996⊗

ABSTRACT: The five cysteines closest to the carboxyl terminus of human ferrochelatase have been individually mutated to serine, histidine, or aspartate residues in an attempt to identify the protein ligands to the [2Fe-2S] cluster. Mutations of cysteines at positions 403, 406, and 411 (C403D, C403H, C406D, C406H, C406S, C411H, and C411S mutants) all resulted in inactive enzyme that failed to assemble the [2Fe-2S] cluster as judged by whole-cell EPR studies. In contrast, mutation of the cysteines at positions 360 and 395 to serines (C360S and C395S mutants) did not affect the enzymatic activity, and the resulting enzyme assembled a [2Fe-2S] cluster that was spectroscopically indistinguishable from the wild-type enzyme. The results indicate that three of the conserved cysteines in the 30-residue C-terminal extension of mammalian ferrochelatase are involved in ligating the [2Fe-2S] cluster. Resonance Raman and variable-temperature magnetic circular dichroism studies of heme-free preparations of human ferrochelatase are reported, and the spectra are best interpreted in terms of one non-cysteinyl, oxygenic ligand for the [2Fe-2S] cluster. Such anomalous coordination could account for the cluster lability compared to similar clusters with complete cysteinyl ligation and hence may be intrinsic to the proposed regulatory role for this cluster in mammalian ferrochelatases.

The final step in the biosynthesis of heme in animal cells represents the convergence of the tetrapyrrole biosynthetic pathway and the cellular iron accumulation and metabolism pathway. This step, the insertion of ferrous iron into the macrocycle, protoporphyrin IX, is catalyzed by the enzyme ferrochelatase (protoheme ferrolyase, EC 4.99.1.1) (Dailey, 1990, 1996)). This enzyme is nuclear-encoded and synthesized in the cytoplasm before being translocated to the matrix side of the inner mitochondrial membrane and proteolytically processed to the mature form (Karr & Dailey, 1988; Camadro & Labbe, 1988). Ferrochelatase has been cloned, expressed, and purified from a variety of sources including yeast (Labbe-Bois, 1990), mouse (Brenner & Fraiser, 1991; Taketani et al., 1990), human (Nakahigashi et al., 1990), bovine (Shibuya et al., 1995), *Escherichia coli* (Miyamoto et al., 1991), *Bradyrhizobium japonicum* (Frustaci & O'Brian, 1992), *Bacillus subtilis* (Hansson & Hederstedt, 1992), *Arabidopsis thaliana* (Smith et al., 1994), and barley and cucumber (Miyamoto et al., 1994). With these sequences and the expression of the mammalian enzyme in *E. coli*, it has become possible to examine a number of naturally occurring mutations (Dailey et al., 1994b) as well as to produce specific site-directed mutants.

The availability of an efficient expression system has also allowed the production and isolation of relatively large amounts of recombinant ferrochelatase, thereby facilitating biophysical characterization of the enzyme. Initial spectroscopic studies of recombinant human and mouse ferrochelatases yielded the surprising result that mammalian, but not yeast or prokaryotic, ferrochelatase contains a $[2Fe\text{-}2S]^{2+,+}$ cluster (i.e., [2Fe-2S] cluster capable of cycling between the +2 and +1 core oxidation levels) that is essential for enzymatic activity (Dailey et al., 1994a; Ferreira et al., 1994). While this cluster is quite labile and breaks down during *in vitro* storage, it is possible to isolate ferrochelatase via a rapid purification procedure with stoichiometric amounts of the [2Fe-2S] cluster (Dailey et al., 1994a; Sellers et al., 1996). Moreover, the lability of the cluster may be intrinsic to its function, since recent studies have suggested a NO-sensing role for the cluster, whereby ferrochelatase activity is regulated via cluster degradation as part of an immune response system (Sellers et al., 1996).

The objectives of this work were to identify the specific residues involved in ligating the [2Fe-2S] in mammalian ferrochelatase. To this end, we have extended our spectroscopic investigations of the [2Fe-2S] cluster in recombinant human ferrochelatase to include resonance Raman (RR)[1] studies, and investigated the consequences of site-directed mutations of conserved cysteine residues. Nine cysteines are conserved in the three mammalian enzymes for which sequence data are currently available, i.e., bovine, human, and mouse (see Figure 1). None of these nine cysteine residues are conserved in plant, yeast, or bacterial ferrochelatases, which do not contain a [2Fe-2S] cluster, and four

† This work was supported by grants from the National Institutes of Health (DK32303 and DK35898 to H.A.D. and GM51962 to M.K.J.) and by the National Science Foundation Research Training Group Award to the Center for Metalloenzyme Studies (DIR9014281).

* Corresponding author. Telephone: (706) 542-9378. Fax: (706) 542-2353. E-mail: johnson@sunchem.chem.uga.edu.

‡ Department of Chemistry and Center for Metalloenzyme Studies.

§ Department of Microbiology and Center for Metalloenzyme Studies.

⊗ Abstract published in *Advance ACS Abstracts,* December 1, 1996.

[1] Abbreviations: RR, resonance Raman; VTMCD, variable-temperature magnetic circular dichroism; Fd, ferredoxin; S^t, terminal or cysteinyl sulfur; S^b, bridging or inorganic sulfide.

S0006-2960(96)02011-9 CCC: $12.00

are found in a 30-residue C-terminal extension that is present in mammalian but not bacterial ferrochelatases (Dailey et al., 1994a). In this work, mutations involving each of the five cysteines closest to the C-terminus have been constructed and investigated in terms of their ability to assemble a [2Fe-2S] cluster by whole-cell EPR studies and/or EPR and variable-temperature magnetic circular dichroism (VTMCD) studies of dithionite-reduced heme-free enzyme preparations. The spectroscopic and mutagenesis results reported below indicate that only three of the C-terminal cysteines are involved in cluster coordination (Cys403, Cys406, and Cys411) and raise the possibility that the cluster lability may be a consequence of one non-cysteinyl, oxygenic cluster ligand.

MATERIALS AND METHODS

Strains and Plasmids. Recombinant human ferrochelatase, pHDTF20, was maintained and expressed in *E. coli* strain JM109 as previously described (Dailey et al., 1994b). For whole-cell EPR experiments, recombinant human ferrochelatase was expressed in *E. coli* strain DW35 (Δ*frdABCD* and *sdhC::kan*) provided by Dr. Gary Cecchini (VA Medical Center, San Francisco). This strain is devoid of fumarate reductase or succinate dehydrogenase activity, and the cells were grown anaerobically on a glucose/fumarate medium (Schröder et al., 1991).

Construction of Mutants. Site-directed mutagenesis of pHDTF20 was performed using the Transformer Mutagenesis procedure (Clonetech), using the QuikChange protocol (Stratagene), or using PCR with synthetic oligonucleotides containing single-base changes along with a *Pst*I endonuclease restriction site. Oligonucleotides for mutagenesis and for sequencing were synthesized with an Applied Biosystems Model 391 DNA synthesizer. All mutations were verified using the Fmol sequencing kit from Promega Corp. For the C403D, C403H, C406D, C406H, and C406S mutations, antisense oligonucleotides containing altered nucleotides were used with a sense-strand oligonucleotide containing the start site and extending into the 5′-end sequence for human ferrochelatase. The PCR reactions contained 2.5 units of taq polymerase, 10 μL of taq-polymerase buffer, 1 ng of pHDTF20 template, 1 μmol of sense and antisense primers, and 20 μmol of dNTPs in a total volume of 100 μL. PCR products, identified and isolated by agarose gel electrophoresis, were retrieved from the PCR reaction using Geneclean (BIO 101, Inc.) and digested with *Bam*HI and *Pst*I. Digested PCR products were isolated from an agarose gel again using Geneclean (BIO 100, Inc.). These digested PCR products were ligated into *Bam*HI/*Pst*I-digested pHDTF20.

The C411S, C411H, and C395S mutations were produced using both a selection primer, changing an *Sph*I endonuclease restriction site to an *Nhe*I site in the pBTac vector plasmid, and a mutagenic primer containing the specifically altered nucleotides which also served to destroy the *Pst*I restriction site normally present near the 3′-end of human ferrochelatase. The transformer mutagenesis protocol followed the published procedure (Deng & Nickoloff, 1992). By digesting potential mutants with *Pst*I, the plasmids containing the mutagenic primer were selected and easily identified. The C360S mutant was constructed following the QuikChange protocol by Stratagene; 125 ng of two complimentary oligonucleotides, each containing the desired mutation of a single nucleotide, was thermocycled along with 100 ng of wild-type plasmid pHDTF20, 1 μL of 10 mM dNTPs, 5 μL of PFU polymerase buffer, and 2.5 units of PFU polymerase in a total volume of 50 μL. The mixture was heated to 95 °C for 30 s followed by 12 cycles of 95 °C for 30 s, 55 °C for 1 min, and 68 °C for 11 min (Papworth et al., 1996). The resulting PCR reaction was digested with *Dpn*I to nick the original template plasmid (Nelson & McClelland, 1992). Four microliters of the digested reaction was used to transform electrocompetent *E. coli* strain JM109.

Purification. Recombinant wild-type and mutant human ferrochelatases were purified as previously described (Dailey et al., 1994a,b) using the published modifications to remove traces of enzyme-bound heme and porphyrin (Sellers et al., 1996). By increasing the starting material to a 6 L culture and by including a second ammonium sulfate cut at the end of the usual purification procedure, highly concentrated pellets of the purified recombinant ferrochelatase were produced. Ferrochelatase pellets were resuspended to the desired concentration for spectroscopic characterizations in 20 mM HEPES, pH 7.4, with 1% octyl glucoside.

Activity Assays. Ferrochelatase activity was assayed anaerobically using the pyridine hemochromogen assay (Dailey & Fleming, 1983). Ferrous ion and mesoporphyrin (from Porphyrin Products, Logan, UT) were the substrates used in these assays. Protein concentrations were determined by the bicinchoninic acid (BCA) procedure (Pierce Chemical Co.), and by the UV absorption at 278 nm using $\epsilon = 46\,900$ M^{-1} cm^{-1}.

Spectroscopic Characterization of Ferrochelatase. UV−visible absorption spectra were recorded on Shimadzu UV3101PC or Cary 219 spectrophotometers. VTMCD spectra were recorded using Oxford Instruments SM3 or Spectromag 4000 split-coil superconducting magnets (1.5−300 K and 0−7 T) mated to a Jasco J-500C or J-715 spectropolarimeters. The samples used for VTMCD contained 50−55% (v/v) glycerol in order to form an optically transparent glass on freezing. The experimental protocols used in VTMCD studies, namely, accurate temperature and magnetic field measurements, anaerobic sample handling, and assessment of residual strain in the frozen samples, have been described in detail elsewhere (Johnson, 1988; Thomson et al., 1993). X-band EPR spectra were recorded on a Brüker ESP-300E EPR spectrometer fitted with an Oxford Instruments ESR-9 liquid helium flow cryostat. Spin quantitations were carried out under nonsaturating conditions using CuEDTA as the standard. Whole-cell EPR samples were spun down at low rpm, to avoid cell lysis, and then transferred into an anaerobic chamber. The cell pellet was suspended in a solution of 500 mM EPPS, pH 8.4, that contained excess sodium dithionite and then transferred to an EPR tube. No signals were seen for unlysed cells unless a small amount of chloroform was stirred into each EPR tube immediately prior to freezing.

RR spectra were recorded using an Instruments SA Ramanor U1000 spectrometer fitted with a cooled RCA 31034 photomultiplier tube with a 90° scattering geometry. Spectra were recorded digitally using photon counting electronics. Multiple scans were collected and averaged in order to increase the signal to noise ratio. Band positions were calibrated using the excitation frequency and a CCl_4 standard and are accurate to within ± 1 cm^{-1}. Lines from a Coherent Innova 100 10-W argon ion and 200-K2 krypton

FIGURE 1: Amino acid sequence comparison for bovine, human, and mouse ferrochelatases (Brenner & Fraiser, 1991; Taketani et al., 1990; Nakahigashi et al., 1990; Shibuya et al., 1995). Conserved cysteine residues are boxed.

ion lasers were used in this work, and plasma lines were removed using a Pellin-Broca Prism premonochromator. Scattering was collected from the surface of a frozen 10 μL drop of sample using a custom-designed anaerobic sample cell (Drozdzewski & Johnson, 1988) attached to the cold finger of an Air Products Displex Model CSA-202E closed cycle refrigerator. With this system, cryogenic temperatures (17−25 K) are obtained, thus improving spectral resolution and also preventing laser-induced sample degradation.

RESULTS AND DISCUSSION

Several lines of evidence have implicated one or more of the four cysteines near the C-terminus of mammalian ferrochelatase in ligation of the [2Fe-2S] cluster (Dailey et al., 1994a) (see Figure 1). First, bacterial ferrochelatases do not have the [2Fe-2S] cluster or the 30-residue C-terminal extension that is present in mammalian ferrochelatase. Second, the four cysteines are conserved in bovine, mouse, and human ferrochelatases which contain the [2Fe-2S] cluster, but are not present in yeast ferrochelatase which has a C-terminal extension and no [2Fe-2S] cluster. Third, the cluster was not present in an engineered mutant of human ferrochelatase that had a 30-residue truncation at the C-terminus. In order to investigate further the ligands involved in cluster ligation, the consequences of individually mutating each of the five cysteines closest to the C-terminus of human ferrochelatase have been investigated. A total of nine mutants have been constructed and investigated thus far, C360S, C395S, C403D, C403H, C406D, C406H, C406S, C411H, and C411S, and the sequences of the mutant proteins were confirmed by nucleotide sequencing. The rationalization for choosing serine, histidine, or aspartate to replace a cysteine was that each of these residues has been shown to be capable of coordinating a [2Fe-2S] cluster in native or

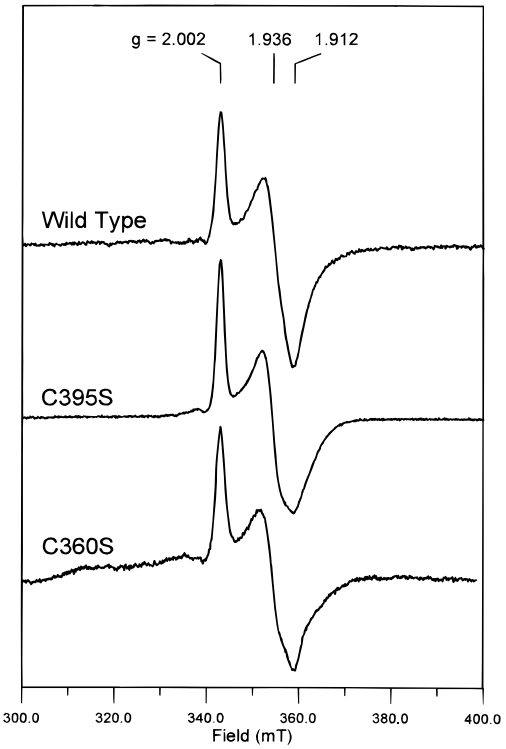

FIGURE 2: X-band EPR spectra of the [2Fe-2S]$^{+}$ centers in dithionite-reduced samples of wild-type, C360S, and C395S recombinant ferrochelatase. The samples, 0.22 mM for the C395S mutant, 0.08 mM for the C360S mutant, and 0.14 mM for the wild type, were in 20 mM HEPES buffer, pH 7.4, with 1% (v/v) octyl glucoside and 10 mM sodium dithionite. EPR conditions: temperature, 35 K; microwave power, 1 mW; microwave frequency, 9.43 GHz; modulation amplitude, 0.64 mT.

mutant samples of other proteins (Gubriel et al., 1989; Werth et al., 1990, 1992; Holden et al., 1993).

Characterization of Mutant Ferrochelatases. Mutant human ferrochelatases were purified from each of the nine variants and investigated by UV−visible absorption (as prepared) and EPR (dithionite-reduced). With the exception of the C360S and C395S mutants, there was no evidence for the presence of [2Fe-2S] clusters in any of the mutant ferrochelatases. The purified samples were colorless and inactive as prepared and exhibited no EPR signals on dithionite reduction. In contrast, the C360S and C395S mutants had activity, UV−visible absorption, and EPR properties indistinguishable from those of the recombinant wild-type enzyme. The absorption spectra of the C360S and C395S mutants were identical to those recently reported for heme-free samples of recombinant ferrochelatase (Sellers et al., 1996), and the EPR spectra for dithionite-reduced samples of wild-type, C360S, and C395S recombinant ferrochelatase are compared in Figure 2. Our initial attempts at spin quantitation with purified samples of recombinant ferrochelatase indicated 0.5−1.0 cluster per monomer and hence could not rule out the possibility of 1 cluster per homodimer rather than 1 cluster per monomer (Dailey et al., 1994a). However, the available evidence indicates that the enzyme is a monomer in solution (Dailey & Fleming, 1983), and the spin quantitations have increased with improvements in the purification procedures and sample handling techniques. The spectra shown in Figure 2 were obtained with samples frozen within 30 s of dithionite reduction and correspond to 0.8−0.9 spin/monomer. Even for samples handled under

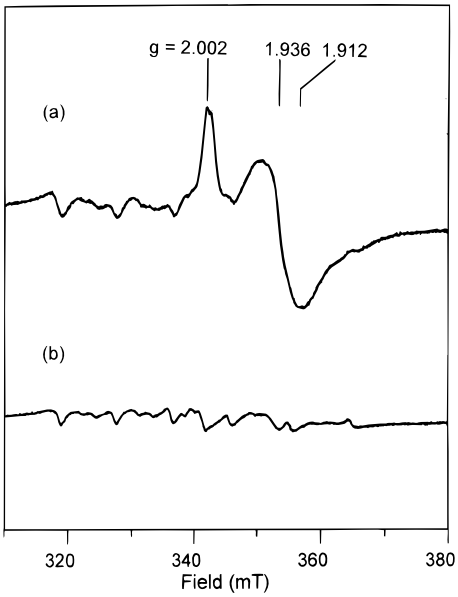

FIGURE 3: X-band EPR spectrum of whole cells of *E. coli* DW35 with (a) and without (b) the plasmid encoding for wild-type ferrochelatase. The unlysed cell pellet was suspended anaerobically in 500 mM EPPS buffer, pH 8.4, with an excess of sodium dithionite, and 10% (v/v) chloroform was added immediately prior to freezing. EPR conditions: temperature, 20 K; microwave power, 1 mW; microwave frequency, 9.60 GHz; modulation amplitude, 0.64 mT.

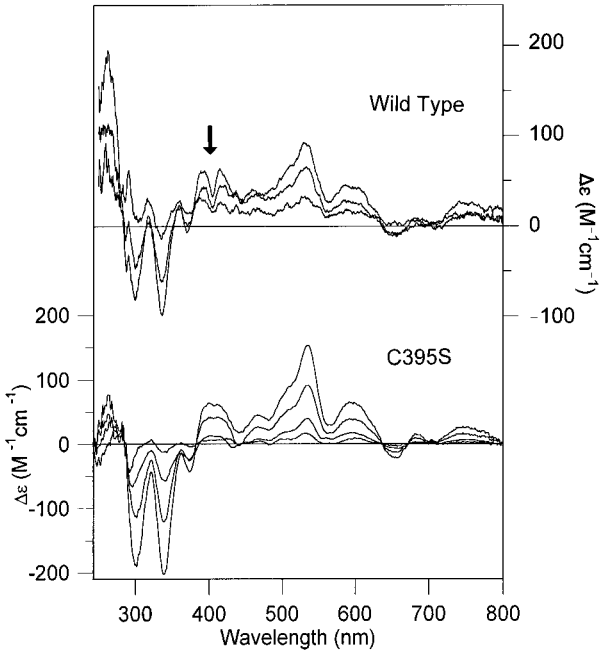

FIGURE 4: VTMCD spectra of dithionite-reduced wild-type and C395S mutant forms of purified recombinant human ferrochelatase. The samples, 0.13 mM for the C395S mutant and 0.08 mM for the wild type, were in 20 mM HEPES buffer, pH 7.4, with 1% (v/v) octyl glucoside and 55% (v/v) glycerol. Each was reduced anaerobically with 20-fold excess sodium dithionite. $\Delta\epsilon$ values are based on the concentration of $S = {}^1/_2$ [2Fe-2S]$^+$ clusters as determined by EPR spin concentrations of identical samples. The spectra were all collected at 4.5 T and 1.66, 4.23, and 9.10 K for the wild type, and 1.65, 4.23, 20.1, and 39.8 K for the C395S mutant. All the bands increase in intensity with decreasing temperature. The arrow in the wild-type spectrum indicates a minor contribution from contaminating heme.

strict anaerobic conditions, the signal intensity decreased at least 5-fold on incubating with dithionite for 30 min. These observations are consistent with one [2Fe-2S]$^+$ cluster per monomer and with enhanced lability for the reduced cluster compared to the oxidized cluster.

The mutagenesis experiments suggest that Cys403, Cys406, and Cys411, but not Cys395 or Cys360, are ligands to the [2Fe-2S] cluster and that the presence of the cluster is essential for enzymatic activity. However, in light of the lability of the [2Fe-2S] cluster in purified samples of human ferrochelatase, it is possible that a cluster is assembled in the C403D, C403H, C406D, C406H, C406S, C411H, and C411S mutants *in vivo*, but is lost during purification due to decreased cluster stability. To explore this possibility, we have developed a method for monitoring the EPR spectrum of the [2Fe-2S]$^+$ cluster in whole cells with amplified expression of recombinant ferrochelatase. Initial attempts were impeded by the presence of resonances arising from succinate dehydrogenase in the *E. coli* strain JM109, which interfered with the detection of the EPR signal from overexpressed ferrochelatase. The expression system was therefore transferred into an *E. coli* strain (DW35) that contains a deletion of the fumarate reductase operon (Δ*frd-ABCD*) and a disruption of the succinate dehydrogenase operon (*sdhC::kan*), such that it is devoid of fumarate reductase or succinate dehydrogenase activity, and the cells were grown anaerobically on a glucose/fumarate medium (Schröder et al., 1991). This resulted in a background against which the EPR signal of the [2Fe-2S]$^+$ cluster in ferrochelatase could be detected in dithionite/chloroform-treated whole cell preparations (see Figure 3). The background signal is largely from Mn(II) that is present in the growth medium. Cells with overexpressed wild-type ferrochelatase exhibited an EPR signal indistinguishable from that of the [2Fe-2S]$^+$ cluster in dithionite-reduced purified ferrochelatase, indicating that the cluster environment is unchanged upon purification. However, no EPR signals above background were observed for whole cells with amplified expression of the C403D, C403H, C406D, C406H, C406S, C411H, and C411S mutant forms of ferrochelatase, showing that mutations prevent assembly of the [2Fe-2S] cluster.

Caution must, however, be exercised in concluding that Cys395 and Cys360 are not cluster ligands, solely on the basis of the lack of significant absorption or EPR changes accompanying mutation to serine residues. EPR in particular does not provide a discriminating method for establishing cluster ligation, since the *g*-value anisotropy is determined primarily by the coordination environment of the Fe(II) site of localized valence [2Fe-2S]$^+$ cluster (Gibson et al., 1966; Bertrand & Gayda, 1979; Bertrand et al., 1985). Indeed, there are now several examples in which cysteine to serine mutations involving cysteines that ligate the nonreducible Fe site of a [2Fe-2S]$^+$ cluster result in no significant change in the EPR properties (Werth et al., 1990; Fujinaga et al., 1993; Xia et al., 1996). The optical absorption data are more convincing, since small but significant changes in the visible absorption spectrum have been observed for cysteine-to-serine mutants of all [2Fe-2S]$^{2+}$-containing Fds investigated thus far (Fujinaga et al., 1993; Cheng et al., 1994; Xia et al., 1996). However, the most convincing evidence that Cys395 and Cys360 are not involved with ligating the cluster comes from VTMCD studies of the dithionite-reduced wild-type, C395S, and C360S forms of purified recombinant human ferrochelatase. Figure 4 compares the spectra obtained for wild-type and the C395S mutant. Very similar

spectra, albeit with substantially poorer signal-to-noise, have been obtained in preliminary studies of the C360S mutant (data not shown). VTMCD spectra of wild-type human ferrochelatase have been published previously (Dailey et al., 1994a). However, the spectra shown in Figure 4 are almost free of heme contamination and provide a much clearer assessment of the bands associated with the $S = {}^1/_2$ [2Fe-2S]$^+$ center. The spectra for the wild-type and C395S mutants are identical except for minor differences in the region between 400 and 450 nm that arise from a trace amount of heme contaminant in the wild type. Taken together, the EPR, VTMCD, and absorption data show that mutation of Cys360 or Cys395 has no effect on the electronic or magnetic properties of the [2Fe-2S] cluster. Moreover, they rule out any possibility of cysteine ligand swapping, via cluster-driven protein conformational change, as observed for cysteine mutants of *Clostridium pasteurianum* 2Fe Fd (Golinelli et al., 1996) and *Azotobacter vinelandii* 7Fe Fd (Martin et al., 1990).

Analysis of the VTMCD Spectra of Dithionite-Reduced Human Ferrochelatase. The VTMCD spectra of Fe-S centers provide an exquisitely sensitive probe of the excited state electronic structure of clusters with paramagnetic ground states. Each electronic transition gives rise to positive or negative absorption-shaped MCD bands that increase in intensity with decreasing temperature. A comparison of the VTMCD of reduced wild-type human ferrochelatase with representative examples of each of three classes of Fd-type [2Fe-2S]$^+$ centers (each having complete cysteinyl ligation), *i.e., S. oleracea* Fd (plant-type), *P. putida* Fd (hydroxylase-type), and *C. pasteurianum* 2Fe Fd, is shown in Figure 5. Assignments of the VTMCD spectra of the reduced Fds have been made, based on comparisons with spectra for oxidized and reduced rubredoxins, and resonance Raman excitation profiles (Fu et al., 1992). Charge transfer transitions involving the localized-valence Fe(II) and Fe(III) sites are assigned to bands between 250−350 and 350−525 nm, respectively. The positive MCD band in the 530−560 nm region, which correlates with a pronounced feature in the corresponding absorption spectrum, is tentatively assigned to a Fe(II) → Fe(III) intervalence transition, and the lower energy bands (<600 nm) are assigned to ligand field transitions. While the close similarity in the Fe(II) → S region between human ferrochelatase and these Fds (*C. pasteurianum* 2Fe Fd in particular) attests to complete cysteinyl coordination at the Fe(II) site, there are marked differences in S → Fe(III) charge transfer region. The overall pattern of positive and negative bands in the S → Fe(III) charge transfer region is particularly invariant among the three classes of Fds, represented in Figure 5a−c, and this is believed to a be a direct consequence of a distorted tetrahedral sulfur environment (i.e., complete cysteinyl coordination) at the localized valence Fe(III) site. Hence, anomalous coordination at the localized valence Fe(III) site is the most likely candidate for distinctive VTMCD properties of the [2Fe-2S]$^+$ cluster in mammalian ferrochelatase.

These electronic assignments and the possibility of one non-cysteinyl ligand for the [2Fe-2S] cluster in mammalian ferrochelatase are generally supported by VTMCD studies of reduced Rieske proteins which have histidyl coordination at the Fe(II) site and cysteinyl coordination at the Fe(III) site,[2] and of cysteine-to-serine mutants of plant- and hydroxylase-type Fds.[3] To illustrate the sensitivity of the

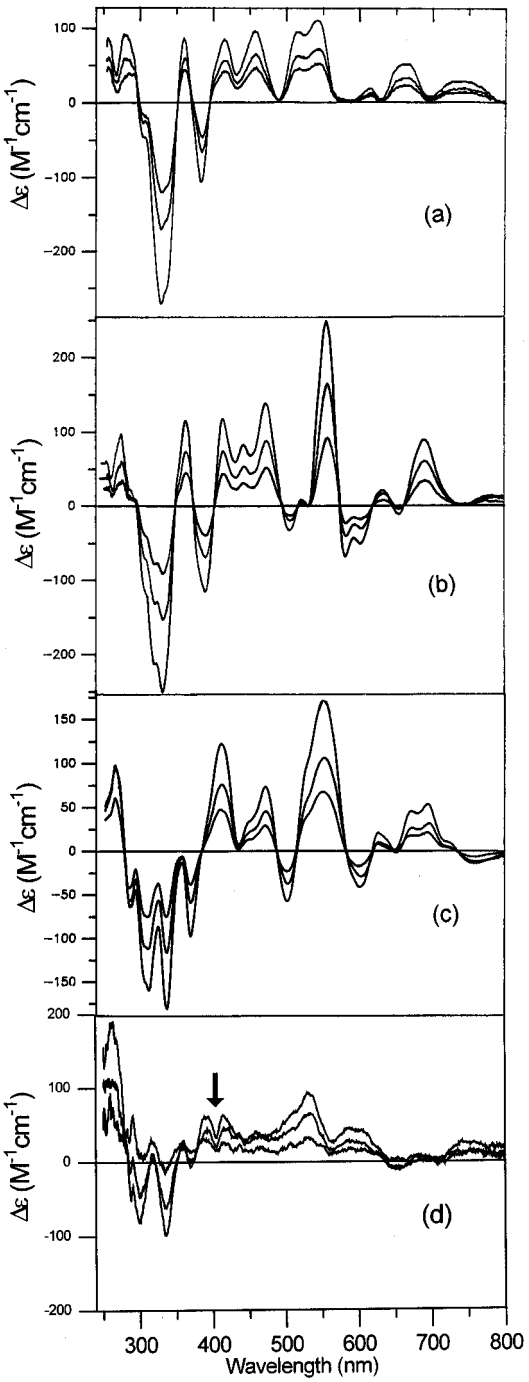

FIGURE 5: Comparison of the VTMCD spectra of dithionite-reduced recombinant human ferrochelatase (d) with three classes of [2Fe-2S]$^+$ Fds: *S. oleracea* Fd (a), *P. putida* Fd (b), and *C. pasteurianum* 2Fe Fd (c). Spectra were recorded in 1-mm cuvettes with a magnetic field of 4.5 T, at temperatures of ~1.6, 4.2, and ~7.0 K; the intensity of all transitions increases with decreasing temperature. The protein samples, 0.23 mM for *S. oleracea* Fd, 0.31 mM for *P. putida* Fd, 0.28 mM for *C. pasteurianum* 2Fe Fd, and 0.08 mM for human ferrochelatase, were in 50 mM Tris/HCl buffer, pH 7.8, with 1 mM mercaptoethanol (a, b, and c) or 20 mM HEPES, pH 7.4, with 1% octyl glucoside (d). All samples contained 50% (v/v) ethylene glycol (a, b, and c) or 55% (v/v) glycerol (d), and were reduced with a 20-fold excess of sodium dithionite. The arrow in the ferrochelatase spectrum indicates a minor contribution from contaminating heme.

VTMCD spectrum in the S → Fe(III) charge transfer region to the ligation at the Fe(III) site, Figure 6 compares spectra obtained for dithionite-reduced wild-type and C55S/C95A[4] mutant forms of human 2Fe Fd (Akin, 1996). The EPR

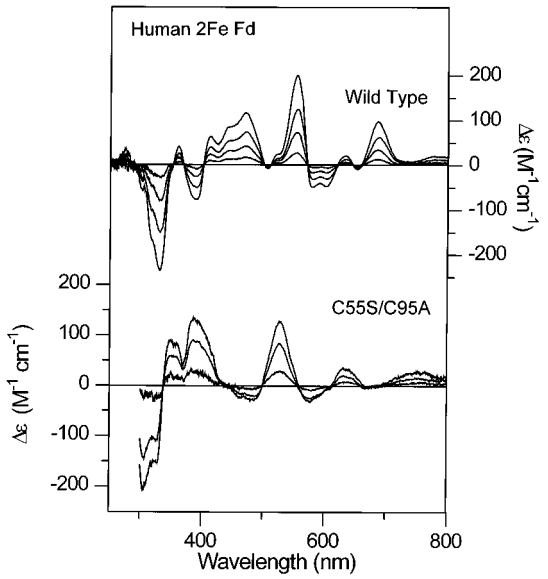

FIGURE 6: VTMCD spectra of dithionite-reduced wild-type and C55S/C95A mutant forms of human 2Fe Fd. Spectra were recorded in 1-mm cuvettes with a magnetic field of 6.0 T, at temperatures of 1.5, 4.2, 10, 20, and 50 K; the intensity of all transitions increases with decreasing temperature. The samples, 0.22 M in Fd, were in 50 mM Tris/HCl buffer, pH 7.8, with 50% (v/v) glycerol, and were supplied by B. Xia and J. L. Markley.

properties of this hydroxylase-type [2Fe-2S]$^{+}$ cluster ($g_{\|} = 2.03$ and $g_{\perp} = 1.94$) are not perturbed by the C55S/C95A mutation, in accord with Cys55 ligating the Fe(III) site. This is confirmed by the VTMCD spectra which show dramatic changes in the S → Fe(III) charge transfer region. While the overall pattern and sign of the bands in this region are not identical to those of the [2Fe-2S]$^{+}$ center in human ferrochelatase, both do show a general simplification of the VTMCD spectrum in this region, suggesting the possibility that an oxygenic ligand might be responsible for the anomalous VTMCD properties in both cases.

Resonance Raman Studies of Human Ferrochelatase. Resonance Raman spectroscopy in the Fe-S stretching region provides a sensitive structural probe for both oxidized and reduced [2Fe-2S] clusters and an independent spectroscopic criterion for assessing the possibility of non-cysteinyl coordination for the cluster in human ferrochelatase. Reliable vibrational assignments have been made based on IR and RR studies of crystallographically defined model complexes and isotopically labeled ferredoxins (Fu et al., 1992; Han et al., 1989a,b). For oxidized [2Fe-2S]$^{2+}$ clusters, the Fe-S stretching frequencies are extremely sensitive to the nature of the coordinating ligands (Kuila et al., 1992; Meyer et al., 1994; Akin 1996) as well as the conformation of coordinating cysteine residues (Fu et al., 1992; Han et al., 1989a,b). Recently it has been shown that the RR spectra of reduced [2Fe-2S]$^{+}$ clusters provide a selective probe of the ligation at the localized valence Fe(III) site. Unfortunately, due to large fluorescence backgrounds, all efforts to obtain RR spectra of dithionite-reduced human ferrochelatase have so

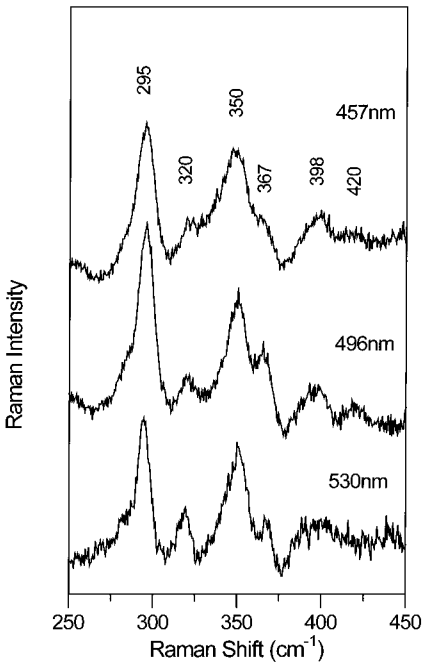

FIGURE 7: Resonance Raman spectrum of recombinant human ferrochelatase as prepared. The excitation wavelengths in nanometers are indicated for each spectrum. The sample, ~0.9 mM, was in 20 mM HEPES buffer, pH 7.4, with 1% ocytl glucoside. All the spectra are the sums of 60 scans, and a linear ramp base line has been subtracted to correct for the fluorescence background. The sample temperature was 25 K, and the spectrometer was advanced in 0.5 cm^{-1} increments, photon counting for 1 s/point with 6 cm^{-1} spectral resolution. Bands originating from the frozen buffer solution have been subtracted from each spectrum after normalizing the intensities of the "ice-band" at 230 cm^{-1}.

far been unsuccessful. However, good quality data have been obtained for the [2Fe-2S]$^{2+}$ cluster in human ferrochelatase as prepared and analysis in light of the available data for wild-type and mutant [2Fe-2S]-containing proteins does afford some insight into the cluster ligation.

RR spectra of human ferrochelatase at several excitation wavelengths are shown in Figure 7, and the spectrum obtained with 457-nm excitation is compared under identical conditions with those of representative examples of each of the three classes of all-cysteine-ligated Fd-type [2Fe-2S]$^{2+}$ centers, *i.e.*, *S. oleracea* Fd (plant-type), *P. putida* Fd (hydroxylase-type), and *C. pasteurianum* 2Fe Fd in Figure 8. The ferrochelatase spectrum is tentatively assigned under effective D_{2h} symmetry in terms of modes primarily involving Fe-S^{b} or Fe-S^{t} stretching by direct analogy with the published assignments for these three Fds (see Table 1). The only uncertainty lies in the assignment of the A_g^t, $B_{3u}{}^b$, and the near-degenerate $B_{1u}{}^t$,$B_{2g}{}^t$ modes (in-phase and out-of-phase combinations of asymmetric Fe-S^{t} modes). The latter modes are not assigned in ferrochelatase since they are generally only observable with violet (413 or 406 nm) excitation lines in 2Fe Fds (Fu et al., 1992; Han et al., 1989a,b). Unfortunately, very high fluorescence backgrounds prevented the acquisition of good quality RR spectra for human ferrochelatase with 406-nm excitation. Isotope shift data for clusters reconstituted with ^{34}S at the bridging position provide the most reliable criterion for assigning the A_g^t and $B_{3u}{}^b$ modes, but it has not yet been possible to effect reconstitution of the cluster in ferrochelatase. Consequently, the assignment in Table 1 is based on the observation that the A_g^t mode invariably occurs at a lower frequency and

[2] T. A. Link, B. R. Crouse, M. G. Finnegan, J. A. Fee, and M. K. Johnson, manuscript in preparation.

[3] B. R. Crouse, L. A. Akin, B. Xia, H. Cheng, J. L. Markley, and M. K. Johnson, manuscript in preparation.

[4] Cys95 is not a cluster ligand in human Fd and was mutated to Ala to avoid possible complications with cluster-driven protein reorganization.

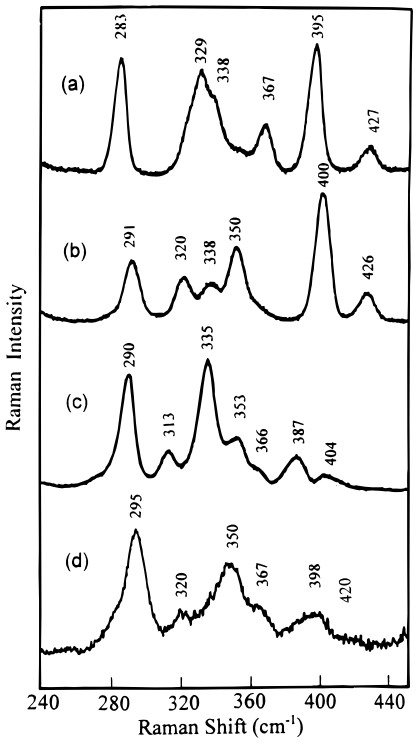

FIGURE 8: Comparison of the resonance Raman spectra of oxidized human ferrochelatase (d) with three classes of $[2Fe\text{-}2S]^{2+}$ Fds: *S. oleracea* Fd (a), *P. putida* Fd (b), and *C. pasteurianum* 2Fe Fd (c). For each sample, the cluster concentration was 1−2 mM, and all were in 50 mM Tris/HCl buffer, pH. 7.8, with 1 mM mercaptoethanol (a, b, and c) or 20 mM HEPES buffer, pH 7.4, with 1% octyl glucoside (d). The spectra were recorded at 17−25 K and are the sum of 6−10 scans except for human ferrochelatase which is the sum of 60 scans. Each scan involved advancing the spectrometer in 0.2 cm^{-1} increments and photon counting for 1 s/point with 6-cm^{-1} spectral resolution. Bands originating from the frozen buffer solution have been subtracted from each spectra after normalizing the intensities of the "ice-band" at 230 cm^{-1}, and a linear ramp fluorescence background has been subtracted from human ferrochelatase data.

Table 1: Fe-S Stretching Frequencies (cm^{-1}) and Assignments for the $[2Fe\text{-}2S]^{2+}$ Centers in *S. oleracea* Fd, *P. putida* Fd, *C. pasteurianum* 2Fe Fd, and Human Ferrochelatase

mode,[a] D_{2h}	*S. oleracea* Fd[b]	*P. putida* Fd[b]	*C. pasteurianum* 2Fe Fd[b]	human ferrochelatase
$B_{2u}{}^{b}$	427	426	404	420
$A_g{}^{b}$	395	400	387	398
$B_{3u}{}^{b}$	367	350	366	367
$B_{1u}{}^{t}$,$B_{2g}{}^{t}$	357[c]	344[c]	353	
$A_g{}^{t}$	338	338	335	350
$B_{1g}{}^{b}$	329	320	313	320
$B_{3u}{}^{t}$	283	291	290	295

[a] Symmetry labels under idealized D_{2h} symmetry for the oxidized $Fe_2S_2{}^{b}S_4{}^{t}$ unit. [b] Assignments taken from Fu et al. (1992). [c] Observed with 406-nm excitation.

generally exhibits stronger enhancement with green/yellow (∼530 nm) excitation, as compared to the $B_{3u}{}^{b}$ mode, in other proteins and model systems (Fu et al., 1992; Han et al., 1989a,b).

The differences in the vibrational frequencies of the three classes of all-cysteine-ligated Fd-type $[2Fe\text{-}2S]^{2+}$ clusters have been attributed to minor variations in Fe−S bond strengths and in differences in the cysteine $Fe\text{-}S^{t}\text{-}C_{\beta}\text{-}C_{\alpha}$ dihedral angles (Fu et al., 1992; Han et al., 1989a,b). However, the anomalously high frequencies assigned to the predominantly Fe-S^{t} stretching modes of the $[2Fe\text{-}2S]^{2+}$ center in ferrochelatase are unlikely to arise from differences in dihedral angles, since the frequency separation between $A_g{}^{t}$ and $B_{3u}{}^{t}$ modes (55 cm^{-1}) is the same as in *S. oleracea* Fd. Recent RR studies of cysteine-to-serine mutant forms of *C. pasteurianum* Fd (Meyer et al., 1994), human Fd (hydroxylase-type) (Akin, 1996), and *Anabaena* 7170 vegetative Fd (plant-type)[3] show that these Fe-S^{t} stretching frequencies can be readily explained by invoking oxygenic coordination in the form of a serinate ligand. While a distinct Fe-O stretching mode (expected in the 540−600 cm^{-1} region) has yet to be observed in any of these mutants, the partial oxygenic ligation is manifest by significant upshifts in both the $B_{3u}{}^{t}$ and $A_g{}^{t}$ modes. For $[2Fe\text{-}2S]^{2+}$ clusters with complete cysteinyl coordination (as judged by structural, mutagenesis, and/or spectroscopic criteria), these modes occur in the ranges 281−291 cm^{-1} and 326−340 cm^{-1}, respectively (Han et al., 1989a; Fu et al., 1992, 1994; Crouse et al., 1994; Moshiri et al., 1995; Zhelyaskov et al., 1995; Akin, 1996). The $B_{3u}{}^{t}$ and $A_g{}^{t}$ Fe-S^{t} stretching modes in human ferrochelatase are assigned at 295 and 350 cm^{-1}, respectively, well outside the ranges established for complete cysteinyl ligation, but within the ranges established for clusters with one serinate ligand, i.e., 289−302 cm^{-1} and 332−351 cm^{-1}, respectively (Meyer et al., 1994; Akin, 1996).[3] It should be noted that similar spectroscopic properties might be expected for other oxygenic ligands such as aspartate or water/hydroxide, but there is as yet no VTMCD or RR data for a [2Fe-2S] cluster with aspartate or water/hydroxide in place of one of the cysteinate ligands. However, the RR data argue against histidine as the noncysteinyl ligand, since the larger effective mass of the imidazole ring would be expected to decrease the frequency of the Fe-S^{t} stretching modes. This is borne out by studies of Rieske-type proteins which have their lowest energy stretching mode near 270 cm^{-1} (Kuila et al., 1992).

CONCLUSIONS

The combination of site-directed mutagenesis coupled with spectroscopic characterization strongly implicates Cys403, Cys406, and Cys411 as ligands to the [2Fe-2S] cluster in human ferrochelatase and demonstrates conclusively that Cys360 and Cys395 are not cluster ligands. While the four additional cysteines that are conserved among mammalian ferrochelatases (Cys31, Cys196, Cys236, and Cys323) are still potential candidates for the fourth cluster ligand, the available VTMCD and RR data for human ferrochelatase can be interpreted in terms of one oxygenic cluster ligand, e.g., serinate, aspartate, or water/hydroxide. Partial noncysteinyl ligation would provide an attractive rationalization for the lability of this cluster compared to [2Fe-2S] clusters with complete cysteinyl coordination, and hence could be intrinsic to the proposed regulatory role as an NO sensor (Sellers et al., 1996). Further mutagenesis, spectroscopic, and structural studies are planned to address the identity of the fourth cluster ligand.

ACKNOWLEDGMENT

We thank Dr. Gary Cecchini, VA Medical Center and the University of California at San Francisco, for providing *E. coli* strain DW35 used in the whole-cell EPR studies and

Dr. John Markley, University of Wisconsin at Madison, for the samples of wild-type and mutant forms of human Fd.

REFERENCES

Akin, L. A. (1996) M.S. Dissertation, University of Georgia.

Bertrand, P., & Gayda, J.-P. (1979) *Biochim. Biophys. Acta 579*, 107−121.

Bertrand, P., Guigliarelli, B., Gayda, J.-P., Beardwood, P., & Gibson, J. F. (1985) *Biochim. Biophys. Acta 831*, 261−266.

Brenner, D. A., & Fraiser, F. (1991) *Proc. Natl. Acad. Sci. U.S.A. 88*, 849−853.

Camadro, J.-M., & Labbe, P. (1988) *J. Biol. Chem. 263*, 11675−11682.

Cheng, H., Xia, B., Reed, G. H., & Markley, J. L. (1994) *Biochemistry 33*, 3155−3164.

Crouse, B. R., Yano, T., Finnegan, M. G., Yagi, T., & Johnson, M. K. (1994) *J. Biol. Chem. 269*, 21030−21036.

Dailey, H. A. (1990) in *Biosynthesis of Heme and Chlorophylls* (Dailey, H. A., Ed.) pp 123−161, McGraw-Hill Publishing Co., New York.

Dailey, H. A. (1996) *Adv. Inorg. Biochem.*, 77−98.

Dailey, H. A., & Fleming, J. E. (1983) *J. Biol. Chem. 258*, 11453−11459.

Dailey, H. A., Finnegan, M. G., & Johnson, M. K. (1994a) *Biochemistry 33*, 403−407.

Dailey, H. A., Sellers, V. M., & Dailey, T. A. (1994b) *J. Biol. Chem. 269*, 390−395.

Deng, W. P., & Nickoloff, J. A. (1992) *Anal. Biochem. 200*, 81−88.

Drozdzewski, P. M., & Johnson, M. K. (1988) *Appl. Spectrosc. 42*, 1575−1577.

Ferreira, G. C., Franco, R., Lloyd, S. G., Pereira, A. S., Moura, I., Moura, J. J. G., & Huynh, B. H. (1994) *J. Biol. Chem. 269*, 7062−7065.

Frustaci, J. M., & O'Brian, M. (1992) *J. Bacteriol. 174*, 4223−4229.

Fu, W., Drozdzewski, P. M., Davies, M. D., Sligar, S. G., & Johnson, M. K. (1992) *J. Biol. Chem. 267*, 15502−15510.

Fu, W., Jack, R. F., Morgan, T. V., Dean, D. R., & Johnson, M. K. (1994) *Biochemistry 33*, 13455−13463.

Fujinaga, J., Gaillard, J., & Meyer, J. (1993) *Biochem. Biophys. Res. Commun. 194*, 104−111.

Gibson, J. F., Hall, D. O., Thornley, J. H. M., & Whatley, F. R. (1966) *Proc. Natl. Acad. Sci. U.S.A. 56*, 987−990.

Golinelli, M.-P., Akin, L. A., Crouse, B. R., Johnson, M. K., & Meyer, J. (1996) *Biochemistry 35*, 8995−9002.

Gubriel, R. J., Batie, C. J., Sivaraja, M., True, A. E., Fee, J. A., Hoffman, B. M., & Ballou, D. P. (1989) *Biochemistry 28*, 4861−4871.

Han, S., Czernuszewicz, R. S., Kimura, T., Adams, M. W. W., & Spiro, T. G. (1989a) *J. Am. Chem. Soc. 111*, 3505−3511.

Han, S., Czernuszewicz, R. S., & Spiro, T. G. (1989b) *J. Am. Chem. Soc. 111*, 3496−3504.

Hansson, M., & Hederstedt, L. (1992) *J. Bacteriol. 174*, 8081−8093.

Holden, H. M., Jacobson, B. L., Hurley, J. K., Tollin, G., Oh, B.-H., Skjeldal, L., Chae, Y. K., Cheng, H., Xia, B., & Markley, J. L. (1993) *J. Bioenerg. Biomembr. 26*, 67−87.

Johnson, M. K. (1988) *ACS Symp. Ser. 372*, 326−342.

Karr, S. R., & Dailey, H. A. (1988) *Biochem. J. 254*, 799−803.

Kuila, D., Schoonover, J. R., Dyer, R. B., Batie, C. T., Ballou, D. P., Fee, J. A., & Woodruff, W. H. (1992) *Biochim. Biophys. Acta 1140*, 175−183.

Labbe-Bois, R. (1990) *J. Biol. Chem. 265*, 7278−7282.

Martin, A. E., Burgess, B. K., Stout, C. D., Cash, V. L., Dean, D. R., Jensen, G. M., & Stephens, P. J. (1990) *Proc. Natl. Acad. Sci. U.S.A. 87*, 598−602.

Meyer, J., Fujinaga, J., Gaillard, J., & Lutz, M. (1994) *Biochemistry 33*, 13642−13650.

Moshiri, F., Crouse, B. R., Johnson, M. K., & Maier, R. J. (1995) *Biochemistry 34*, 12973−12982.

Miyamoto, K., Nakahigashi, Y., Nishimura, K., & Inokuchi, H. (1991) *J. Mol. Biol. 219*, 393−398.

Miyamoto, K., Tanaka, R., Teramoto, H., Masuda, T., Tsuji, H., & Inokuchi, H. (1994) *Plant Physiol. 105*, 769−770.

Nakahigashi, Y., Taketani, S., Okuda, M., Inoue, K., & Tokunaga, R. (1990) *Biochem. Biophys. Res. Commun. 173*, 748−755.

Nelson, M., & McClelland, M. (1992) *Methods Enzymol. 216*, 279−303.

Papworth, C., Braman, J., & Wright, D. A. (1996) *Stratagies 4*, 34−35.

Schröder, I., Gunsalus, R. P., Ackrell, B. A. C., Cochran, B., & Cecchini, G (1991) *J. Biol. Chem. 266*, 13572−13579.

Sellers, V. M., Johnson, M. K., & Dailey, H. A. (1996) *Biochemistry 35*, 2699−2704.

Shibuya, H., Nonneman, D., Tamassia, M., Allphin, O. L., & Johnson, G. S. (1995) *Biochim. Biophys. Acta 1231*, 117−120.

Smith, A. G., Santana, M. A., Wallace-Cook, A. D. M., Roper, J. M., & Labbe-Bois, R. (1994) *J. Biol. Chem. 269*, 13405−13413.

Taketani, S., Nakahigashi, Y., Osumi, T., & Tokunaga, R. (1990) *J. Biol. Chem. 265*, 19377−19380.

Thomson, A. J., Cheesman, M. R., & George, S. J. (1993) *Methods Enzymol. 226*, 199−232.

Werth, M. T., Cecchini, G., Manodori, A., Ackrell, B. A., Schroder, I., Gunsalus, R. P., & Johnson, M. K. (1990) *Proc. Natl. Acad. Sci. U.S.A. 87*, 8965−8969.

Werth, M. T., Sices, H., Cecchini, G., Schroder, I., Lasage, S., Gunsalus, R. P., & Johnson, M. K. (1992) *FEBS Lett. 299*, 1−4.

Xia, B., Cheng, H., Bandarian, V., Reed, G. H., & Markley, J. L. (1996) *Biochemistry 35*, 9488−9495.

Zhelyaskov, V., Yue, K. T., LeGall, J., Barata, B. A. S., & Moura, J. J. G. (1995) *Biochim. Biophys. Acta 1252*, 300−304.

BI9620114